Original

Investigation of Temperature Evolution and Flash Formation at AA5083 Studs During Friction Surfacing

Zina Kallien[1,a], Lars Rath[1,b], Arne Roos[1,c], and Benjamin Klusemann[1,2,d]

[1]Institute of Materials Research, Materials Mechanics, Solid State Joining Processes, Helmholtz-Zentrum Geesthacht, Geesthacht, Germany.

[2]Institute of Product and Process Innovation, Leuphana University of Lüneburg, Lüneburg, Germany.

[a]zina.kallien@hzg.de, [b]lars.rath@hzg.de, [c]arne.roos@hzg.de, [d]benjamin.klusemann@hzg.de

Abstract. Friction surfacing (FS), a solid-state joining process, is a coating technology for metallic materials. Frictional and plastic deformation enable the deposition of a consumable material on a substrate. Process temperatures stay below the melting point of the consumable material and are an important factor determining the quality of the resulting deposit. The focus of the current study is the experimental analysis of the flash formation and the temperature evolution in consumable studs during FS deposition of dissimilar aluminum alloys. The main process parameters, axial force, rotational speed and travel speed, were varied while the setting of the process surrounding was kept constant. The temperature evolution for the applied process parameter combinations are investigated for the stud material via infrared camera. The results show that the choice of applied force, rotational speed and travel speed did not lead to significant changes in maximum process temperature values of the consumable stud detectable via infrared camera. However, the flash formation at the tip of the plasticized stud shows significant differences for varied process parameters. Especially reduction of travel speed or increase in axial force led to formation of larger flashes. Since the material that is pressed out of the process zone into the flash is not deposited on the substrate, the flash formation can be linked to the material efficiency of the FS process.

Introduction

The processing of superior lightweight structures demands for highly developed processing technologies. The prominent aim is to keep and improve material properties during the joining of different materials. The solid-state technologies are an alternative to conventional fusion-based processes for joining of similar and dissimilar materials. For solid-state processes, the temperature is below the materials' melting point throughout the joining process. Due to the absence of material fusion and solidification, undesirable material reactions with regarding the mechanical performance are avoided. The reduced heat input also leads to less distortion and residual stresses.

Friction surfacing (FS) belongs to the solid-state joining processes and represents a coating technology. An axial force is applied on a rotating consumable stud which is pressed onto a substrate. Heat develops due to friction leading to plasticization of the material at the stud's tip. When a relative movement between plasticized stud and substrate starts, a layer of the plasticized consumable material is deposited on the substrate.

The process parameters rotational speed, axial force and travel speed, are crucial for the quality of the deposit. The trends in resulting deposit geometry for changes in process parameters are known from former studies, summarized in the review by Gandra et al. [1]. Higher forces result in reduced deposit thickness and width [2–5]. The same trend was observed for increased rotational speeds [5–10]. An increase in travel speed also leads to a reduction in deposit thickness and width [2,6,11,12]. The choice of process parameters is strongly dependent on the materials that are supposed to be processed since

the necessary energy input depends on thermal properties of the materials [13]. Hanke and dos Santos [13] detected the highest temperature during the process in the shear zone between stud and deposit. Higher temperatures were detected comparing the deposition of AA 6082 and AA 5083 consumable stud material. This finding pronounces the importance of material parameters for the FS process. A change in process parameters has a direct an influence on the process temperature. Increased process temperatures were measured in the substrate for increased rotational speeds [14–16] and axial feeding rates [14, 16]. Higher travel speeds were found to lead to lower process temperatures [14, 16, 17]. However, experimental investigations of process temperature distribution directly in the process zone, at the interface between substrate and plasticized stud material, is difficult. But, the temperature is of significant importance for the FS process. The relation between process parameters as well as material parameters and process temperature is complex. To address this aspect, thermal analyses via infrared camera of the process were performed in order to observe the spatial process temperature evolution with focus on the stud material and investigating the resulting flash formation.

Experimental Setup

In the present study, AA 5083 was used as consumable stud material (20 mm diameter, 125 mm length). The stud is rotating at rotational speeds between 900 rpm and 1500 rpm. The stud is pressed on an AA 7050 substrate material (300 mm length, 130 mm width, 10 mm thickness) with an axial force of 6 kN to 10 kN. When the tip of the stud plasticizes, the process-typical flash is formed. The flash is formed by plasticized material which is pressed out of the process zone. The amount of flash that is pushed into the flash influences the material efficiency [19]. The machine table is moving at travel speeds of 4 mm/s to 8 mm/s, enabling the deposition of plasticized stud material onto the substrate. Between machine table and substrate, an additional AA 7050 backing plate (300 mm length, 130 mm width, 8 mm thickness) was used. The used studholder material was X37 tool steel. The total welding path was 140 mm long.

The focus of the present study lies on the influence of the main process parameters axial force, rotational speed and travel speed, on the temperature evolution and distribution in the stud. For this, the process surroundings as substrate material and thickness, stud material, backing material and thickness as well as studholder material are kept constant.

The process temperature evolution was recorded by an infrared camera (Image IR 8300, InfraTec, Germany) with focus on the stud at a frame rate of 20 Hz. The recorded thermograms are investigated with regard to plasticizing behavior and maximum temperature value when the process is in steady state, i. e. after 70 mm of deposition. The flash formation is also observable in the thermograms and will be compared for the different process parameter combinations. In order to compare the resulting flash geometries, the diameter of the flash was measured for the remaining studs. Additionally, the minimum and maximum flash height of the remaining studs were measured to assess the regularity of the formed flash. The detailed flash analysis can be performed from cross sections of the remaining studs.

Results and Discussion

The temperature evolution along with the plasticizing behavior of the stud material is recorded by the infrared camera as shown in Fig. 1. The thermograms of the process show a sudden rise in temperature within the first seconds when the rotating stud gets in contact with the substrate's surface. Frictional heat occurs at the materials' interface and the consumable material starts to deform and material plasticization is initiated while further heating of the consumable stud occurs. When the tip of the stud is plasticized, the temperature in the contact zone between stud and substrate reaches a stable value and the process becomes steady state. When this phase is reached, no further heating in the contact zone can be observed via infrared camera. This behavior was also reported in former studies [20, 21]. Rafi et al. [21] mentioned that the attainment of the steady state during deposition, which is a result of

viscous heat dissipation during plastic deformation, can be assumed as adiabatic because of the short duration. After the process becomes steady state at the tip, a slow heat accumulation within the stud and flash is observed for increased process duration.
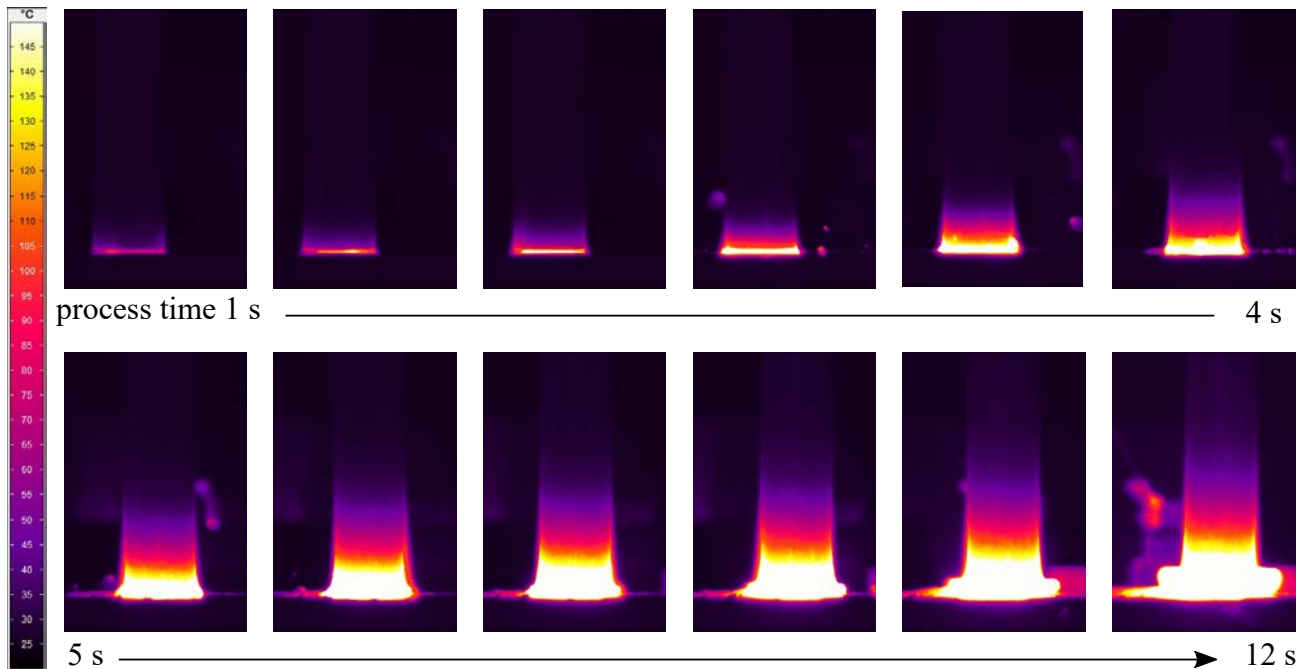

Fig. 1: Thermograms of an FS stud material during the start of the plasticizing behavior for process parameters of 8 kN applied force, 1200 rpm rotational speed and 6 mm/s travel speed.

A change in FS process parameters leads to a change in the energy input during the deposition. The process temperature distribution in the studs is compared after a welding distance of 70 mm, where the process is assumed steady state. The thermograms for the applied process parameter combinations are shown in Fig. 2. The maximum temperature values were detected at the tip of the plasticized stud at the interface to the deposit, which agrees well with the observations in the literature [13]. No significant difference in the temperature distribution as well as maximum temperature value could be observed from the thermograms for the different process parameters. Since the energy input to the process is changed by adapting the process parameters, significant temperature differences are expected. Due to the rotational movement and the material flow at the tip of the consumable stud material, the outside of the stud cools down fast due to heat transfer to the environment. Furthermore, the infrared camera is only able to record the outside of the processing zone. The results indicate that initial temperature differences directly at the plasticized tip do not affect the temperature in the flash material, detectable by the infrared camera. Overall, the temperature distributions reached a steady state, which is independent of possible changes in energy input within the parameter window of this study.

The difference in process parameters has most probably a significant influence on the material flow behavior. This is visible by the flash formation at the tip of the stud, also observable from the thermograms. Additionally, the remaining studs' cross sections are shown in Fig. 2 to illustrate the flash formation in detail. The flash diameter as well as the deviation of flash height measured for the remaining studs after welding are displayed in Fig. 3 for varying process parameters. For the variation in rotational speed, no significant difference in flash geometry was observed. One thing to point out is that for reduced rotational speed an irregular flash of distinct deviation in height developed. Regarding the influence of travel speed, the process with 4 mm/s showed increased flash height and diameter compared to travel speeds of 6 mm/s and 8 mm/s. For constant welding distances, the travel speed determines the process duration. During long processes more plasticized material is enabled to

be pressed out of the process zone and to form the flash. So, the process of the longest duration, i. e. lowest travel speed, showed the largest flash. Interestingly, no significant difference in flash formation could be observed comparing the travel speeds 6 mm/s and 8 mm/s. It is assumed that there is a minimum amount of flash formation that is dependent on the applied force. The higher the applied force, the more flash develops. The rise in force increased flash height and diameter significantly Fig. 3(c). The developed flash for 10 kN applied force was of very irregular height which can clearly be seen from the cross section (Fig. 2(j)) where an applied process force led to a very low amount of flash of approximately no deviation in height (Fig. 2(k)). By changing axial force, the axial material feeding rate is changed, which determines the pressure on the plasticized stud material. High axial forces lead to a larger amount of plasticized material that is pressed out of the process zone into the flash. This probably also influences the speed of material flow, resulting in a different flash formation behavior. Process duration and material flow are changed by variation in process parameters resulting in a different behavior in flash formation. Therefore, after the same welding distance of 140 mm, the remaining studs for reduced travel speeds and increased applied forces are significantly shorter than the remaining studs for other process parameter combinations. For a detailed material efficiency analysis, the geometry of deposited material has to be taken into account which is not scope of the present study.
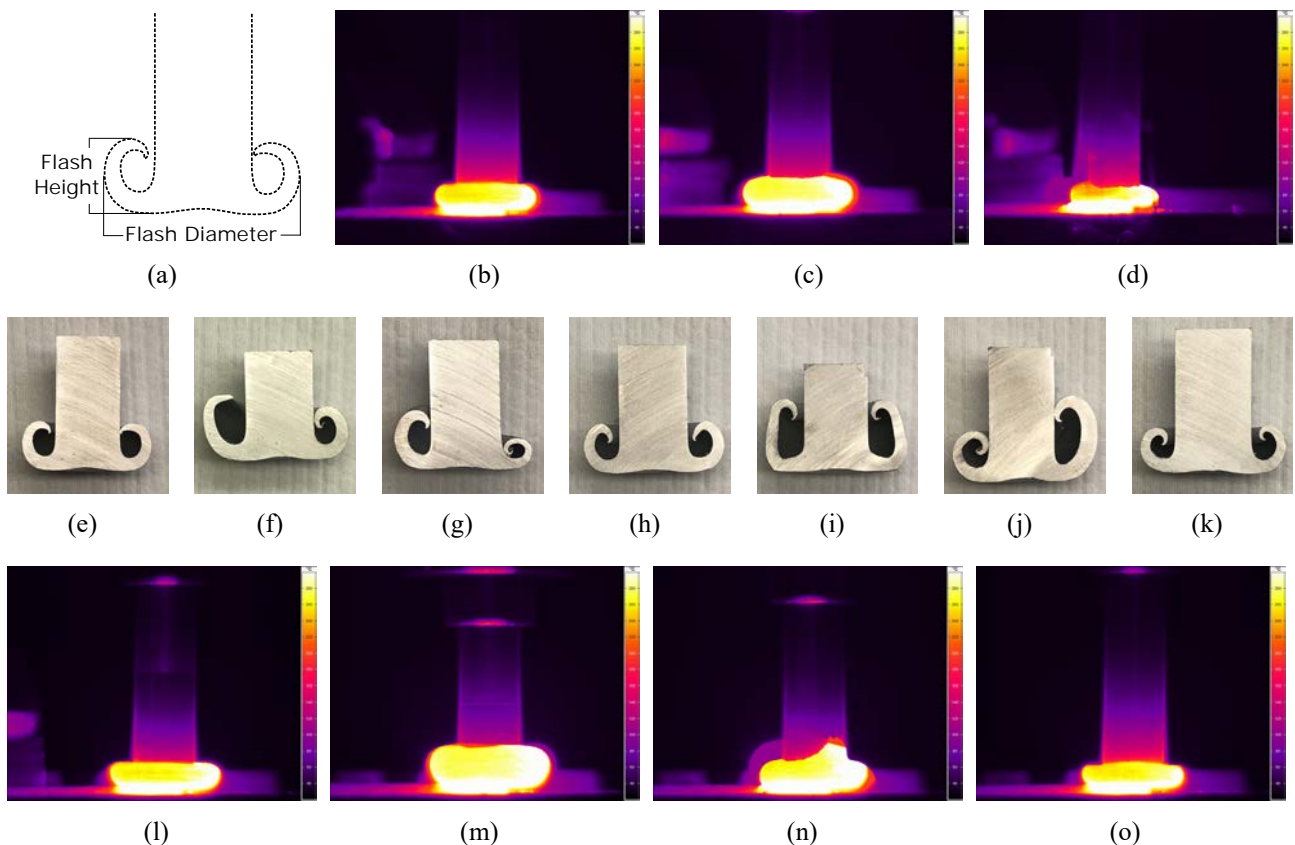

Fig. 2: Schematic stud cross section (a); thermograms at 70 mm welding distance and cross section of remaining studs after 140 mm welding distance; 8 kN-1200 rpm-6 mm/s (b) and (e), 8 kN-1500 rpm-6 mm/s (c) and (f), 8 kN-900 rpm-6 mm/s (d) and (g), 8 kN-1200 rpm-8 mm/s (l) and (h), 8 kN-1200 rpm-4 mm/s (m) and (i), 10 kN-1200 rpm-6 mm/s (n) and (j) and 6 kN-1200 rpm-6 mm/s (o) and (k).
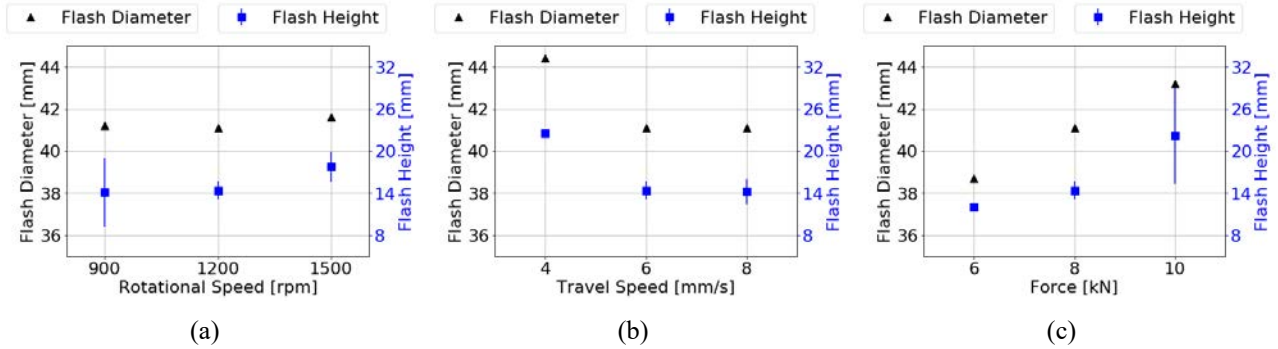
Fig. 3: Flash height and diameter measured for remaining studs after 140 mm welding distance for variation of rotational speed (a), travel speed (b) and axial force (c).

Summary and Conclusion

In the present study, the FS process was investigated via infrared camera for varied process parameters. Resulting thermograms of the stud material were compared and analyzed at half of the total performed welding distance, i. e. in steady state. With regard to the maximum temperature value detected by the infrared camera, no significant difference could be observed for different process parameter combinations due to rapid cooling from the material flow into the flash. Additionally, the FS of aluminum alloys requires a comparably low heat input and the components are of high heat conductivity. The absent temperature difference for different parameter combinations might also allow the assumption that the recorded temperature value is the temperature at which the used material combination is in steady state. However, the flash formation at the tip of the stud is different for the varied process parameters, especially for changes in axial force and travel speed indicating that the material flow is influenced. The applied force and the process duration are assumed to determine the amount of material that is enabled to form the flash during the material deposition.

References

[1] J. Gandra, H. Krohn, R. M. Miranda, P. Vilaça, L. Quintino, and J. F. Dos Santos. Friction surfacing—a review. *Journal of Materials Processing Technology*, 214(5):1062–1093, 2014.

[2] V. I. Vitanov and I. I. Voutchkov. Process parameters selection for friction surfacing applications using intelligent decision support. *Journal of Materials Processing Technology*, 159(1):27–32, 2005.

[3] J. Gandra, D. Pereira, R. M. Miranda, and P. Vilaça. Influence of process parameters in the friction surfacing of aa 6082-t6 over aa 2024-t3. *Procedia CIRP*, 7:341–346, 2013.

[4] D. Govardhan, A.C.S. Kumar, K.G.K. Murti, and G. Madhusudhan Reddy. Characterization of austenitic stainless steel friction surfaced deposit over low carbon steel. *Materials & Design (1980-2015)*, 36:206–214, 2012.

[5] Javed Akram, Prasad Rao Kalvala, and Mano Misra. Effect of process parameters on friction surfaced coating dimensions. *Advanced Materials Research*, 922:280–285, 2014.

[6] H. Khalid Rafi, G. D. Janaki Ram, G. Phanikumar, and K. Prasad Rao. Friction surfaced tool steel (h13) coatings on low carbon steel: A study on the effects of process parameters on coating characteristics and integrity. *Surface and Coatings Technology*, 205(1):232–242, 2010.

[7] S. Mohanasundaram, S. J. Vijay, and M. Karthikeyan. A review on developing surface composites using friction surfacing. *Applied Mechanics and Materials*, 852:402–410, 2016.

[8] Dai Nakama, Kazuyoshi Katoh, and Hiroshi Tokisue. Some characteristics of az31/az91 dissimilar magnesium alloy deposit by friction surfacing. *Materials Transactions*, 49(5):1137–1141, 2008.

[9] Hidekazu Sakihama, Hiroshi Tokisue, and Kazuyoshi Katoh. Mechanical properties of friction surfaced 5052 aluminum alloy. *MATERIALS TRANSACTIONS*, 44(12):2688–2694, 2003.

[10] B. Vijaya Kumar, G. Madhusudhan Reddy, and T. Mohandas. Influence of process parameters on physical dimensions of aa6063 aluminium alloy coating on mild steel in friction surfacing. *Defence Technology*, 11(3):275–281, 2015.

[11] D. Govardhan, K. Sammaiah, K.G.K. Murti, and G. Madhusudhan Reddy. Evaluation of bond quality for stainless steel-carbon steel friction surfaced deposits. *Materials Today: Proceedings*, 2:3511–3519, 2015.

[12] H. Khalid Rafi, G. D. Janaki Ram, G. Phanikumar, and K. Prasad Rao, editors. *Friction surfacing of austenitic stainless steel on low carbon steel: Studies on the efects of traverse speed*, volume 2184 of *Lecture notes in engineering and computer science*, 2010.

[13] S. Hanke and J. F. Dos Santos. Comparative study of severe plastic deformation at elevated temperatures of two aluminium alloys during friction surfacing. *Journal of Materials Processing Technology*, 247:257–267, 2017.

[14] Parisa Pirhayati and Hamed Jamshidi Aval. An investigation on thermo-mechanical and microstructural issues in friction surfacing of al–cu aluminum alloys. *Materials Research Express*, 6(5), 2019.

[15] V. Fitseva, S. Hanke, and J. F. Dos Santos. Influence of rotational speed on process characteristics, material flow and microstructure evolution in friction surfacing of ti-6al-4v. *Materials and Manufacturing Processes*, 32(5):557–563, 2016.

[16] Zahra Rahmati, Hamed Jamshidi Aval, Salman Nourouzi, and Roohollah Jamaati. Modeling and experimental study of friction surfacing of aa2024 alloy over aa1050 plates. *Materials Research Express*, 6(8), 2019.

[17] S. Hanke, P. Staron, T. Fischer, V. Fitseva, and J. F. Dos Santos. A method for the in-situ study of solid-state joining techniques using synchrotron radiation - observation of phase transformations in ti-6al-4v after friction surfacing. *Surface and Coatings Technology*, 335:355–367, 2017.

[18] H. Krohn, S. Hanke, M. Beyer, and J. F. Dos Santos. Influence of external cooling configuration on friction surfacing of aa6082 t6 over aa2024 t351. *Manufacturing Letters*, 5:17–20, 2015.

[19] Pedro Vilaça, Hannu Hänninen, Tapio Saukkonen, and Rosa M. Miranda. Differences between secondary and primary flash formation on coating of hss with aisi 316 using friction surfacing. *Welding in the World*, 58(5):661–671, 2014.

[20] X. M. Liu, Z. D. Zou, Y. H. Zhang, S. Y. Qu, and X. H. Wang. Transferring mechanism of the coating rod in friction surfacing. *Surface and Coatings Technology*, 202(9):1889–1894, 2008.

[21] H. Khalid Rafi, Krishnan Balasubramaniam, G. Phanikumar, and K. Prasad Rao. Thermal profiling using infrared thermography in friction surfacing. *Metallurgical and Materials Transactions A*, 42(11):3425–3429, 2011.